Accepted Manuscript

Grain refinement of wire arc additively manufactured titanium by the addition of silicon

S. Mereddy, M.J. Bermingham, D.H. StJohn, M.S. Dargusch

PII: S0925-8388(16)33516-2

DOI: 10.1016/j.jallcom.2016.11.049

Reference: JALCOM 39544

To appear in: *Journal of Alloys and Compounds*

Received Date: 29 September 2016

Accepted Date: 4 November 2016

Please cite this article as: S. Mereddy, M.J. Bermingham, D.H. StJohn, M.S. Dargusch, Grain refinement of wire arc additively manufactured titanium by the addition of silicon, *Journal of Alloys and Compounds* (2016), doi: 10.1016/j.jallcom.2016.11.049.

Grain Refinement of Wire Arc Additively Manufactured Titanium by the Addition of Silicon

S. Mereddy, M.J. Bermingham, D.H. StJohn and M.S. Dargusch
School of Mechanical and Mining Engineering and Queensland Centre for Advanced Materials Processing and Manufacturing (AMPAM), The University of Queensland, Australia

Author contact details:

Sri Mereddy: sri.mereddy@uqconnect.edu.au

Michael J. Bermingham (corresponding author) m.bermingham@uq.edu.au ; Tel: +61 7 3346 9571

David H. StJohn: d.stjohn@uq.edu.au

Matthew S. Dargusch: m.dargusch@uq.edu.au

ABSTRACT

This study demonstrates that silicon additions are effective in refining the microstructure of additive layer manufactured (ALM) titanium components. The addition of up to 0.75wt% silicon to commercially pure titanium manufactured by wire arc ALM results in a significant reduction of the prior-β grain size. It is observed that silicon also reduces the width of the columnar grains and allows for the nucleation of some equiaxed grains through the development of constitutional supercooling and growth restriction. The grain size of the ALM components is compared to a casting process and it is found that the as-deposited microstructure produced during ALM exhibits larger average grain sizes. Using the Interdependence model for predicting grain size, it was determined that the population of nucleant particles that naturally occur in titanium, has comparable potency (i.e. ability to activate at a similar undercooling) regardless of the processing method, however, the ALM process contains fewer, sufficiently potent, nucleant particles than for the casting process due to the effect of subsequent cycles of remelting and heating.

Keywords: additive manufacturing, grain refinement, titanium, silicon

1. INTRODUCTION

Titanium's high strength to weight ratio, corrosion resistance and ability to withstand high temperatures makes its alloys prime candidates for aerospace applications [1, 2]. The highly desirable properties of titanium such as high ductility, strength and thermal resistance also make it very difficult to machine [1]. Subtractive manufacturing is inefficient in terms of time and material waste. For example, in the F-22 Raptor, an aircraft composed of approximately 39% titanium, only a tenth of the material purchased is used in the aircraft, with the remainder being lost due to machining waste [3]. Additive Layer Manufacturing (ALM) is an emerging net shape forming technology that seeks to address these material wastage issues [4]. ALM processes involve building components from powder or wire through selective melting or sintering in a layer-by-layer fashion [5]. Wire arc ALM is a novel method that allows for greater production rates (several kg/hr) and allows for the bulk production of large components [6].

One key issue preventing the widespread use of additively manufactured products is the fact that the material properties of ALM components can be inferior compared to those of conventionally fabricated products [6]. In titanium alloys, the local solidification of small melt pools during layer deposition can result in epitaxial growth and the formation of columnar grains as heat is primarily extracted through the previously deposited solidified layer, often across a steep thermal gradient [7]. The emergence of grain boundary α that forms during the subsequent solid state transformation along aligned prior-β columnar grains can result in highly anisotropic properties and poor ductility in components produced by ALM [8-11].

The issue of large directional grains can be addressed either with the addition of potent nuclei, a solute that promotes constitutional supercooling or a combination of the two [12, 13]. The Interdependence model clearly shows the interdependence between solute and particle potency in creating an equiaxed structure. Nuclei are naturally present in liquid metals and are the starting point of every grain. Introducing additional potent nucleant particles by inoculation would facilitate grain refinement by increasing the total number of grains and therefore reducing the average grain size [14]. Select growth restricting solutes can promote grain refinement by providing the

constitutional supercooling required to activate nucleant particles. Columnar grain growth occurs parallel to the direction of heat transfer from a pre-existing solid region and must be restricted to obtain homogeneity and to facilitate grain refinement. Constitutional supercooling of the melt pool reduces the growth rate of columnar grains at the solid-liquid interface [12]. This allows for additional nucleation events to take place within the melt thereby increasing the grain density. By using potent nuclei and a solute in unison, grain refinement can be optimised to produce a large number of nucleation events.

The purpose of this study is to improve the microstructure of wire arc additively manufactured titanium to enable wider use of ALM products. Specifically, prior-β grain size reduction is targeted to improve properties such as yield strength, ductility and toughness [15]. Previous research [16-20] has demonstrated that silicon is effective in improving the β-grain density through constitutional supercooling for cast titanium alloys. At the time of writing, there is no commercial grain refining technology available or a clear understanding within the field of the factors that promote effective grain refinement of solidified ALM components. This study aims to address this gap in knowledge by investigating silicon as a grain refiner in the unique solidification conditions experienced by additively manufactured titanium products.

2. METHOD

Wire arc ALM was chosen due to its relatively low cost and fast deposition rates. The apparatus consisted of a EWM Tetrix350 welding machine which acted as the power source needed to melt the raw wire. The wire feedstock was Commercially Pure (CP) ASTM Grade 1 titanium (Baoji Xinnuo Net Metal Materials Co. Ltd, Fe - 0.023wt%, C - 0.009wt%, N - 0.014wt%, O - 0.05wt%, Ti Balance). It was supplied through an automatic Tetrix 4L wire feed unit and was deposited by the welder on to a Ti-6Al-4V base plate. The welder's electrode, the wire feed nozzle and a gas shield were designed to move in unison through the use of a Computer Numerical Control interface. This allowed the system to move in all three dimensions, enabling the fabrication of complex 3D structures. The operating parameters of the apparatus are listed in Table 1.

Table 1. Parameters used during the ALM process

AM Machine Parameters	
Welder Type	Tungsten Inert Gas (TIG)
Electrode	Tungsten–rare earth, 2.4 mm diameter
Welding Current	150 A
Distance between electrode and base plate	5 mm
Titanium Wire Grade (feedstock)	ASTM Grade 1
Wire Diameter	1 mm
Wire Feed Rate	1.5 m/min
Deposition Rate	150 mm/min
Shielding Gas	Argon, 99.999% purity

The ALM machine was used to deposit straight lines of titanium 200 mm in length and approximately 10 mm in width. Ten layers of titanium were deposited for each build for a total of three samples. The first build was a control sample and contained no silicon. Silicon was added to the subsequent two builds through the use of specially prepared silicon paints, in a similar fashion reported elsewhere [21]. Two silicon paints were used for this experiment: one with 25 wt% silicon and another with 40 wt% silicon. Both paints contained an alcohol based gel into which silicon powder was added. The gel was chosen so that it would evaporate quickly upon deposition onto the substrate, leaving only silicon particles behind and minimising possible contamination. Oxidation of the samples was prevented during the deposition process by using a specially designed gas trailing shield to surround the deposited samples with high purity argon gas.

The silicon powder particles used in the paints were less than 1 μm in diameter. This particle size was chosen to allow for rapid dissolution and adequate diffusion within the deposited titanium once melted. To introduce the silicon into the deposited material, the silicon paint was applied prior to the deposition of each layer along the arc's path. The titanium wire feedstock was then deposited over the paint layer where in-situ alloying occurred. This process was repeated for ten layers of deposition. The two silicon paints were used to create two samples: one with low silicon content and the other with high silicon content. Figure 1 shows the components of the ALM machine as well as a partially completed experimental component.

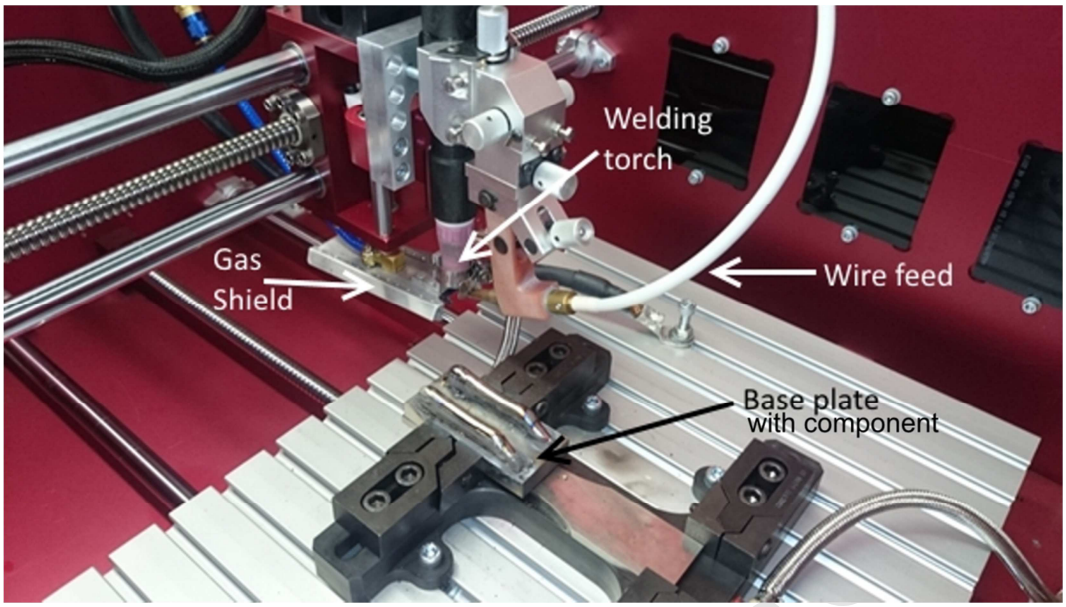

Figure 1. ALM apparatus with welding torch, wire feed and gas shield as well as a titanium component under construction.

After deposition, the samples were stress-relieved for 2 hours at 480°C as per industry standards [2, 22]. Small areas of the samples were cut so that their elemental composition and silicon content could be determined using spectroscopy. The chemical composition of each sample and the feedstock wire is shown in Table 2. There is a small increase in Fe, N and O after deposition compared to the initial wire composition. Following this, three cross-sections were cut from each sample at various locations and were mounted in resin and polished using conventional techniques.

Table 2. Average compositions of ALM samples (wt%).

Silicon Content	Si (%)	Fe (%)	N (%)	O (%)	Ti (%)
Wire Feedstock	-	0.023	0.009	0.05	bal.
None	0.04	0.11	0.04	0.19	bal.
Low	0.19	0.11	0.05	0.17	bal.
High	0.75	0.05	0.03	0.16	bal.

The polished sections were then analysed using microscopy to determine the number of prior-β grains within each section. The conventional ASTM intercept method was not employed to determine grain size for this study due to the directional nature of grain growth. As grain sizes varied depending on the axis of measurement, a variant of the planimetric method [23] was utilised to determine the level of refinement. Using this method all grains were counted manually and grain boundaries were traced on digital photographs to verify the measurements. These outlines were added to allow for easier visualisation of the grain boundaries as they cannot be viewed clearly at low magnifications. This method provides an accurate method for determining the grain size through the sections. Figure 2 compares an unedited image to its enhanced image for reference. The total number of grains within each 2D section was divided by the sample's area to obtain a 2D grain density (grains/mm^2). A total of nine samples were analysed in this manner; three for each level of silicon.

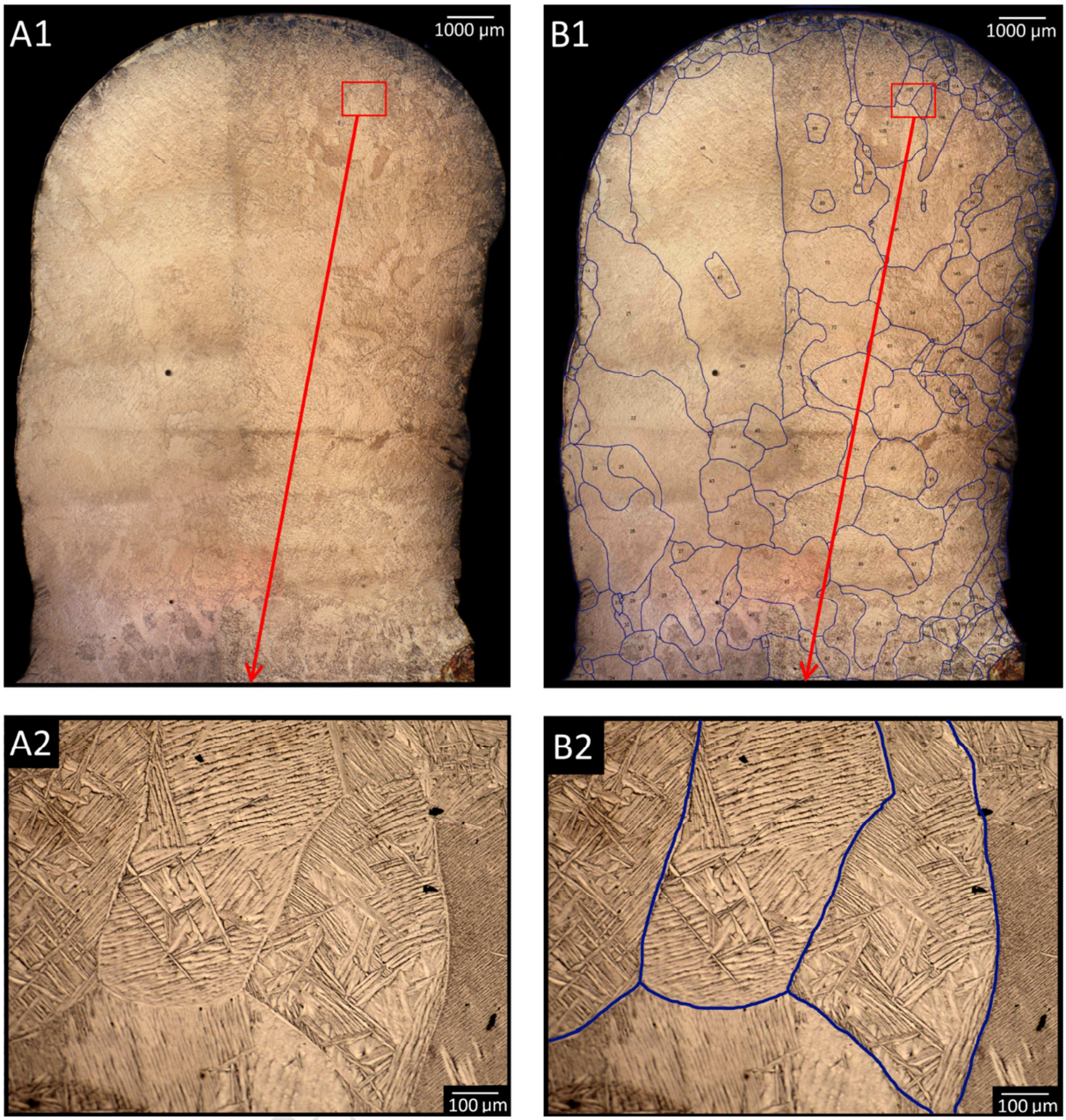

Figure 2. Comparison of raw (A) and enhanced (B) images used in the analysis to enhance visualisation of prior-β grain boundaries and determine the grain size. The prior-β grain boundaries are visible due to the presence of grain boundary-α that forms on these boundaries during the β→α transformation. Within the prior-β grains, the α-phase adopts widmanstätten and colony-α structures [24]. The areas marked by the rectangles in A1 and B2 are shown at a higher magnification in A2 and B2 respectively.

3. Results and Discussion

The technique of using a silicon rich paint and in-situ alloying with the wire feedstock successfully produced a homogenous deposit with no evidence of unalloyed silicon found. Moreover, with in-situ alloying it was determined that the prior-β grain size decreased with increasing silicon content. Figure 3 shows the outlines of the prior-β grain boundaries within three sections of varying silicon

concentration. These results were quantified through the use of 2D grain density measurements (grains/mm^2) and the results are shown in Figure 4.

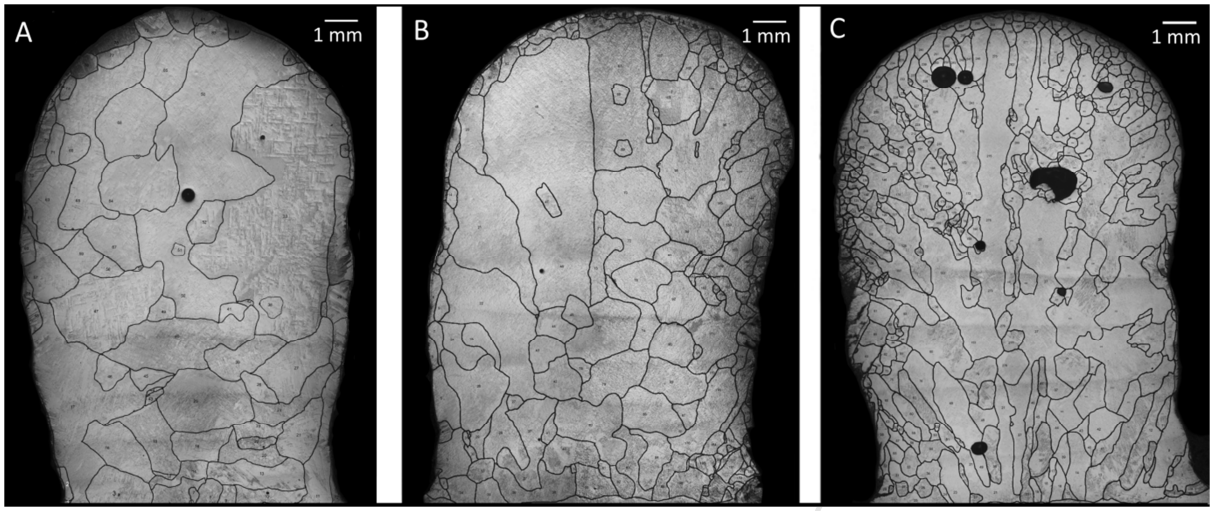

Figure 3. Prior-β grain structure of additive manufactured CP titanium with a) 0.04% Si, b) 0.19% Si and c) 0.75% Si.

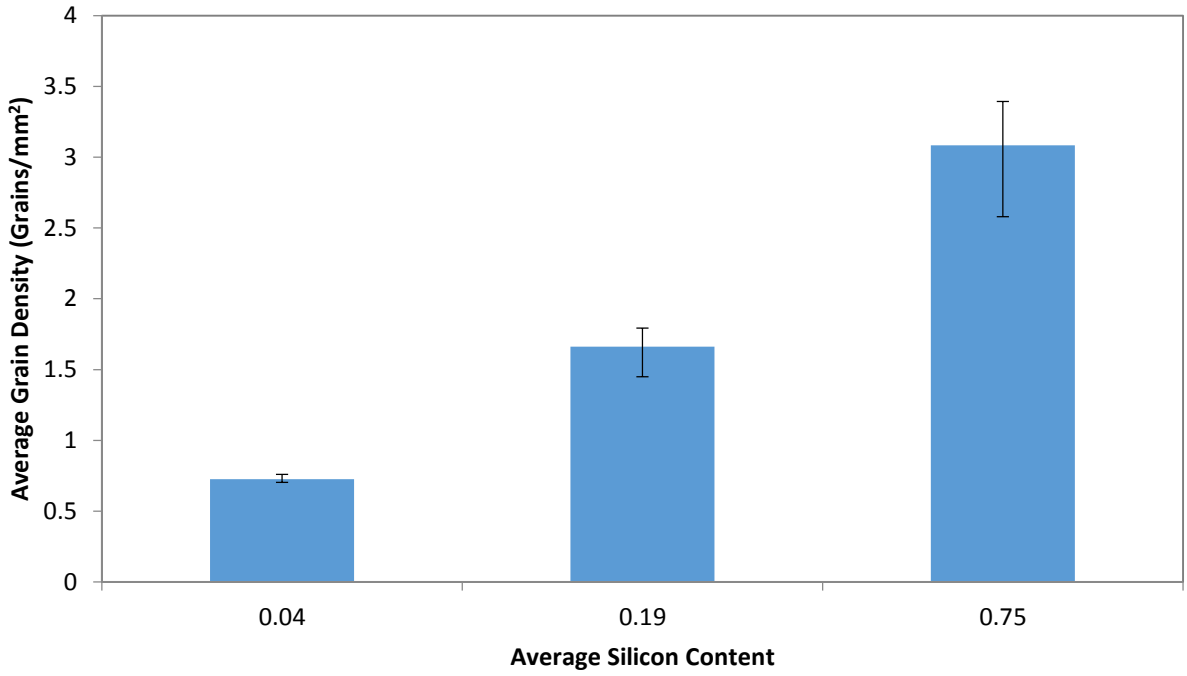

Figure 4. The effect of silicon on the average prior-β grain density of additively manufactured CP titanium. Error bars indicate total range of grain density values.

Figures 3 and 4 indicate a clear decrease in the average size of prior-β grains with increasing silicon concentration. Figure 3 also shows that the grain size is dramatically reduced along the outer edge of each ALM build. This feature may suggest that the surface which has direct contact with the argon atmosphere cools quickly upon deposition forming a chill zone similar to that found in cast microstructures near the mould wall. The presence of an oxide film may also enhance nucleation on the surface. For ALM processes, however, many of these small grains either experience grain growth

from the heat generated by subsequent layer deposition or are remelted. Solidification then occurs epitaxially on grains present in previously formed layers, taking on a columnar structure due to the steep thermal gradients experienced. While columnar growth is also expected in traditionally cast components, it is more prevalent in this ALM processes due to the strong directional heat flow into the base plate creating a steep temperature gradient. It can be seen from Figure 3 that silicon addition reduces the grain size but does not lead to a uniform equiaxed grain size although Figure 3c appears to be a mixture of columnar and equiaxed regions along its length. Silicon's role as a grain refiner is expected to reduce columnar growth by promoting the nucleation of equiaxed grains in constitutionally supercooled zones. Instead, many of the columnar grains become narrower with increased silicon content due to lateral rejection of silicon rich solute slowing growth in this direction thus promoting further nucleation where the columnar structure is initiated. The vertical lengths of the columnar grains remain similar to those of the silicon-free samples. Columnar grain growth is primarily located in the centre of each sample where unidirectional heat flow promotes favourably orientated grain growth in the vertical direction.

The prior-β grain boundaries observed in Figure 3 demonstrate that the microstructures of ALM components differ from those of conventionally manufactured components. The degree of this difference is quantified in Figure 5 which compares the grain refining effects of silicon observed in the current work with results observed for cast microstructures. The average 2D grain density values were used to determine the average grain sizes. Figure 5 shows the relationship between the grain size and the silicon content in comparison with pervious work conducted on castings made with CP titanium by Bermingham et al. [17]. It is apparent from Figure 5 that the additively manufactured samples have larger grain sizes for a similar silicon content.

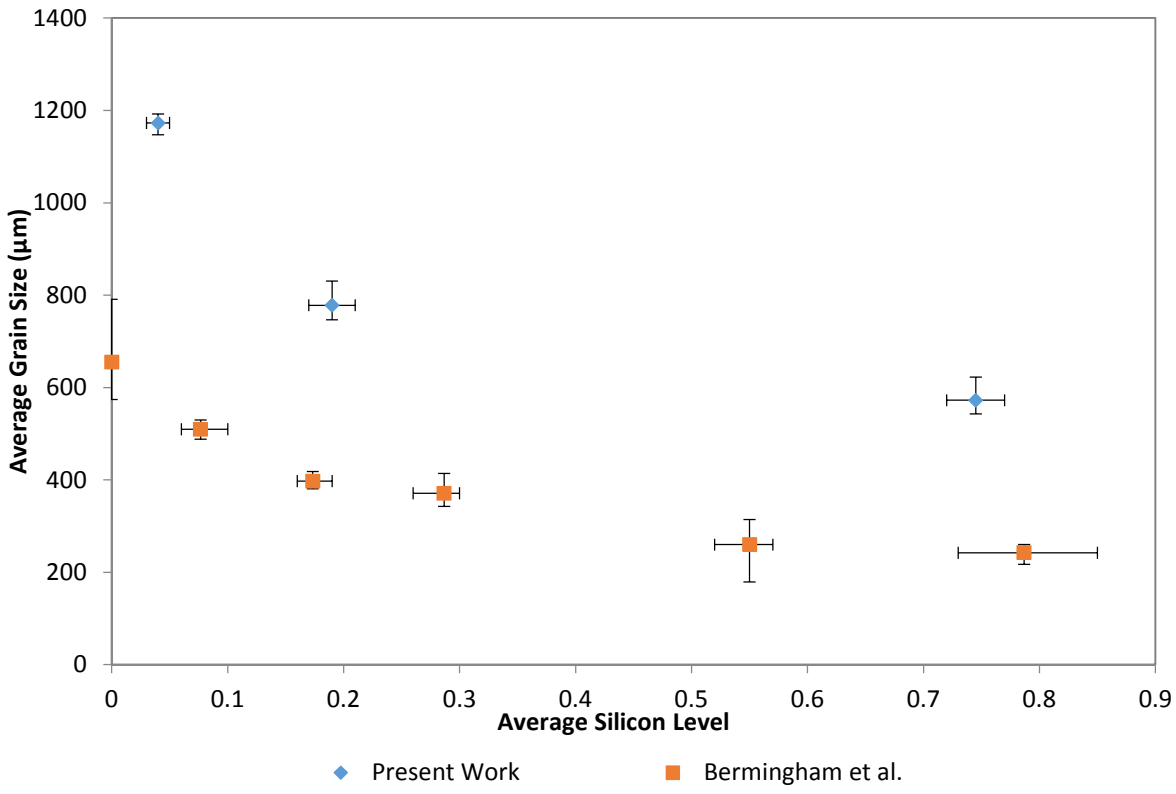

Figure 5. Prior-β grain size versus silicon content on additive manufactured titanium and cast titanium (results obtained from Bermingham et al. [17]). Error bars indicate the range of grain sizes and silicon content for multiple test samples.

The difference in the average grain sizes of the ALM and cast components can be explained by the Interdependence model [25]. This model relates grain size to nucleation parameters and alloy chemistry. Specifically, solute parameters such as the concentration of the alloy, C_o, solute diffusion rate, D, and growth restriction factor, Q, are used in conjunction with nucleant parameters such as the required activation undercooling, ΔT_n, and particle spacing, x_{sd}, to determine the average grain size. This relationship is given by equation 1:

$$d_{gs} = \underbrace{\frac{D\, z\Delta T_n}{vQ} + \frac{4.6D}{v}\left(\frac{C_l^* - C_0}{C_l^*(1-k)}\right)}_{\text{Slope}} + \underbrace{x_{sd}}_{\text{Y - Intercept}} \quad (1)$$

where d_{gs} is the average grain size in micrometres, $z\Delta T_n$ is the incremental amount of undercooling required to re-establish the nucleation undercooling of the most potent nucleant particle, v is the grain growth velocity, C_l^* is the percentage of solute at the solid liquid interface and k is the partition coefficient of the solute. x_{sd} is the distance between the nucleation-free zone defined by the first two terms in equation (1) and the next most potent activated nucleant particle in the melt. Equation 1 assumes a constant particle number density for all compositions. The intercept of the fitted line with the y-axis in Figure 6 is an indication of the size of x_{sd}. In essence, the model indicates that the solidified grain size depends on the presence of a nucleant particle population in the melt (with an average spacing of x_{sd} and each particle requires a critical amount of constitutional supercooling for activation), as well as the presence of a segregating solute that provides the necessary amount of constitutional supercooling (which depends on Q, D and v in equation 1).

For a given composition of silicon solute, D, Q, C_0 and k would be the same for both cast and ALM scenarios, but the different processing conditions could experience different cooling rates which would cause the grain growth velocity (v) to differ. However, despite the differences between the casting and ALM processes, it is found from experimental observation that the growth velocities are reasonably similar. In previous work Bermingham *et al*. investigated the solidification conditions between the ALM process used here and previous casting work by comparing the secondary dendrite arm spacing (SDAS) of boron containing titanium alloys [21]. In both casting [26] and ALM [21] processes it was found that the SDAS was comparable at approximately 25µm, indicating similar cooling rates during solidification. Therefore, from this it is expected that the grain growth velocity (v) at the solid - liquid interface will be comparable given that the cooling rates (defined as the product of thermal gradient and growth velocity) during the casting and ALM processes are similar.

With all other parameters of the Interdependence model being the same or at least similar in value, the remaining factors which may contribute to the discrepancy between the measured ALM and cast grain sizes in Figure 5 are the required nucleation supercooling $z\Delta T_n$ (potency) and the distance between nucleant particles x_{sd}. These two factors depend on the types of nucleant particles present in the melt, their prevalence and whether or not they are activated during solidification.

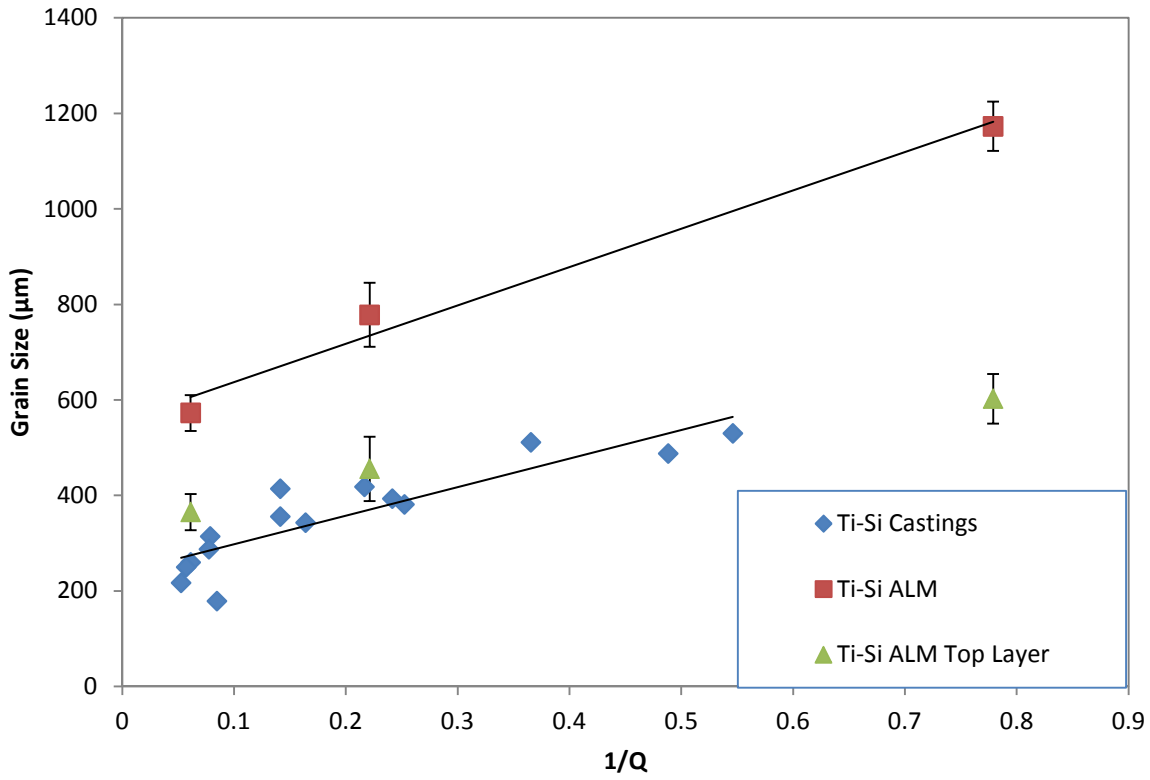

Figure 6. Average prior-β grain size versus the inverse of the growth restriction factor for wire arc additively manufactured and cast titanium-silicon alloys (results obtained from Bermingham et al. [17]). Silicon content is inversely proportional to 1/Q. Error bars indicate ± 1 standard deviation for multiple test samples.

Figure 6 plots the relationship between the average grain size against the inverse of the growth restriction factor (1/*Q*) for the ALM and cast samples. It has been found that in general the gradient of the trend lines (i.e. the slope calculated by first terms in Equation 1) indicates the relative potency of the nucleant particles and the intercept is x_{sd} related to the maximum number of activatable particles [27]. The gradients of the two trend lines are similar, visually confirming that the parameters defining the slope of Equation 1 are similar for both the cast and ALM cases. Given that all other parameters defining the slope in Equation 1 are comparable, it can be concluded that the potency of the nucleant particles (given by ΔT_n) is also similar for both casting and ALM. The major difference between the ALM and casting processes, however, is the y-intercept value x_{sd}. The x_{sd} parameter is the distance between activated nucleant particles and it is evident that the casting process contains a higher density of nucleant particles than that present during the ALM process (i.e. smaller x_{sd}).

Layer remelting is a phenomenon that may account for the apparent observation that the alloys produced by the ALM process contain fewer activated nucleant particles than alloys produced by the casting process. In Figure 3 it is observed that the finest grains in the ALM parts are often found in the top region, particularly near the top surface layer. When the top of the previously deposited layer remelts during the ALM process by the newly deposited layer, many of the fine equiaxed grains that are present in the original top surface remelt and then on re-solidification grow epitaxially on the existing unmelted solid part of the layer. Furthermore, the additional thermal exposure as a new

layer is deposited may also promote grain growth in the solid below the remelted layer. Both of these scenarios would have the effect of increasing the overall measured grain size. In Figure 6 the grain size for the top final layer (10^{th} layer) has been included and it is clear that the grain size in this region is much smaller than the bulk ALM grain size and is close to the grain size of the cast alloys. It also reaffirms the earlier conclusion that the alloys used during the ALM process likely contain nucleant particles with a comparable potency to those present in the cast alloys.

The magnitude of the destruction of equiaxed grains during remelting provides a valuable insight into the requirements of a refinement technology able to form equiaxed grains during solidification after remelting of each deposited layer. If these naturally occurring nucleant particles can be identified, and more of them introduced during ALM, then smaller grain sizes comparable to the casting process may be achievable. Furthermore, as indicated by equation 1, introducing nucleant particles that activate at lower undercooling (i.e. particles of higher potency with lower ΔT_n) would also result in substantial refinement by increasing nuclei activation rates. The goal of future research is to discover new potent nucleant particles that have the potential to promote a fine equiaxed grain size during ALM even under layer remelting conditions given that nucleation ahead of the solid/liquid interface is essential to prevent epitaxial growth of oriented columnar grains. In titanium castings, Bermingham *et al*. [28] developed a method using titanium powder as an endogenous nucleant which, in conjunction with growth-restricting solute, was effective in reducing the grain size by an order of magnitude. Recently, Wang *et al*. [29] and Zhang *et al*. [30] observed fine equiaxed grains in titanium alloy components manufactured by direct metal deposition (LENS process) under certain processing conditions and concluded that these had nucleated on partially melted powder particles. This demonstrates that the columnar-to-equiaxed transition and refinement of β-grains during ALM is possible if suitable nucleant particles can be introduced.

4. CONCLUSIONS

Silicon was added to wire arc additively manufactured titanium components to refine the size of prior-β grains through constitutional supercooling and growth restriction. It was found that increasing the silicon content results in smaller grain sizes but it does not prevent the formation of columnar grains in the microstructure. Silicon additions refine the width of the columnar grains by a growth restriction process as solute is laterally segregated. By comparing the average grain size measurements with similar alloys produced by casting, it was found that the ALM components contained coarser grains for similar silicon concentrations. Utilising the Interdependence model, it was determined that the activated nucleant particles are the same or have a similar nucleation potency for both solidification conditions, and that the average distances between nucleating particles were much greater for the ALM structures when compared to cast components. This difference indicates that the ALM components contain a lower density of activated nucleant particles compared to the castings. However, it was found that the grain size of the top ALM layer is similar to cast titanium suggesting that the initially formed equiaxed grains are eliminated during layer remelting and subsequent epitaxial columnar growth coarsens the grain size. It can be concluded that the prior-β grain sizes of wire arc additively manufactured titanium components can be controlled by adding silicon but further refinement can only be achieved when potent nucleant particles are added in conjunction with silicon.

ACKNOWLEDGEMENTS

The authors would like to acknowledge the support of the Queensland Centre for Advanced Materials Processing and Manufacturing (AMPAM), the Defence Materials Technology Centre (DMTC), the Australian Research Council's Discovery Program and the Queensland Government's Research Partnership Program.

REFERENCES

[1] X. Yang, C. Richard Liu, Machining titanium and its alloys, Machining Science and Technology, 3 (1999) 107-139.
[2] J.M.J. Donachie, Titanium - A Technical Guide (2nd Edition), in, ASM International.
[3] S. Seong, O. Younossi, B.W. Goldsmith, T. Lang, M. Neumann, Titanium: Industrial Base, Price Trends, and Technology Initiatives, Ebsco Publishing, 2009.
[4] K. Michaels, Aerospace Supply Chain & Raw Material Outlook, in: SpeedNews 4th Aerospace Raw Materials & Manufacturers Supply Chain Conference, SpeedNews, Beverly Hills, California, 2014.
[5] Titanium Technologies Workshop, in, Defence Materials Technology Centre, 2013.
[6] F. Wang, S. Williams, P. Colegrove, A. Antonysamy, Microstructure and Mechanical Properties of Wire and Arc Additive Manufactured Ti-6Al-4V, Metallurgical and Materials Transactions A, 44 (2013) 968-977.
[7] A.A. Antonysamy, J. Meyer, P.B. Prangnell, Effect of build geometry on the β-grain structure and texture in additive manufacture of Ti6Al4V by selective electron beam melting, Materials Characterization, 84 (2013) 153-168.
[8] E. Brandl, B. Baufeld, C. Leyens, R. Gault, Additive manufactured Ti-6Al-4V using welding wire: comparison of laser and arc beam deposition and evaluation with respect to aerospace material specifications, Physics Procedia, 5, Part B (2010) 595-606.
[9] S.H. Mok, G. Bi, J. Folkes, I. Pashby, J. Segal, Deposition of Ti-6Al-4V using a high power diode laser and wire, Part II: Investigation on the mechanical properties, Surface and Coatings Technology, 202 (2008) 4613-4619.
[10] F. Wang, S. Williams, P. Colegrove, A.A. Antonysamy, Microstructure and mechanical properties of wire and arc additive manufactured Ti-6Al-4V, Metallurgical and Materials Transactions A, 44 (2013) 968-977.
[11] B. Baufeld, O.V.D. Biest, R. Gault, Additive manufacturing of Ti-6Al-4V components by shaped metal deposition: Microstructure and mechanical properties, Materials and Design, 31 (2010) S106-S111.
[12] W. Kurz, D.J. Fisher, Fundamentals of solidification, Trans Tech Publications, Aedermannsdorf, Switzerland, 1989.
[13] D.M. Stefanescu, Equilibrium and non-equilibrium during solidification, in: Science and Engineering of Casting Solidification, Second Edition, Springer US, Boston, MA, 2009, pp. 1-20.
[14] H. Fredriksson, U. Åkerlind, Nucleation, in: Solidification and Crystallization Processing in Metals and Alloys, John Wiley & Sons, Ltd, 2012, pp. 166-200.
[15] J. Campbell, Chapter 9 - Structure, defects and properties of the finished casting, in: Castings (Second Edition), Butterworth-Heinemann, Oxford, 2003, pp. 267-305.
[16] J. Zhu, A. Kamiya, T. Yamada, A. Watazu, W. Shi, K. Naganuma, Effect of Silicon Addition on Microstructure and Mechanical Properties of Cast Titanium Alloys, Materials Transactions, JIM, 42 (2001) 336-341.
[17] M.J. Bermingham, S.D. McDonald, M.S. Dargusch, D.H. StJohn, The mechanism of grain refinement of titanium by silicon, Scripta Materialia, 58 (2008) 1050-1053.
[18] J.M. Oh, J.M. Lim, B.G. Lee, C.Y. Suh, S.W. Cho, S.W. Lee, G.S. Choi, Grain Refinement and Hardness Increase of Titanium via Trace Element Addition, Materials Transactions, JIM, 51 (2010) 2009-2012.

[19] K.M. Ibrahim, A.H. Hussein, M. Abdelkawy, Effect of Si-addition as a grain refiner on microstructure and properties of Ti-6Al-4V Alloy, Transactions of Nonferrous Metals Society of China (English Edition), 23 (2013) 1863-1874.
[20] A.M.G. Tavares, W.S. Ramos, J.C.G. de Blas, E.S.N. Lopes, R. Caram, W.W. Batista, S.A. Souza, Influence of Si addition on the microstructure and mechanical properties of Ti-35Nb alloy for applications in orthopedic implants, Journal of the Mechanical Behavior of Biomedical Materials, 51 (2015) 74-87.
[21] M.J. Bermingham, D. Kent, H. Zhan, D.H. St John, M.S. Dargusch, Controlling the microstructure and properties of wire arc additive manufactured Ti-6Al-4V with trace boron additions, Acta Materialia, 91 (2015) 289-303.
[22] F.H. Froes, Titanium: Physical Metallurgy, Processing, and Applications, ASM International, 2015.
[23] ASTM, Standard Test Methods for Determining Average Grain Size, in, ASTM International, West Conshohocken, PA, 2013.
[24] M.J. Bermingham, S.D. McDonald, M.S. Dargusch, D.H. St. John, Microstructures of cast titanium alloys, Materials Forum, 31 (2007) 84 - 89.
[25] D.H. StJohn, M. Qian, M.A. Easton, P. Cao, The Interdependence Theory: The relationship between grain formation and nucleant selection, Acta Materialia, 59 (2011) 4907-4921.
[26] M.J. Bermingham, S.D. McDonald, K. Nogita, D.H. St. John, M.S. Dargusch, Effects of boron on microstructure in cast titanium alloys, Scripta Materialia, 59 (2008) 538-541.
[27] M.A. Easton, D.H. StJohn, An analysis of the relationship between grain size, solute content, and the potency and number density of nucleant particles, Metallurgical and Materials Transactions A, 36 (2005) 1911 - 1920.
[28] M.J. Bermingham, S.D. McDonald, D.H. StJohn, M.S. Dargusch, Titanium as an endogenous nuclei, Philosophical Magazine, 90 (2010) 699 - 715.
[29] T. Wang, Y.Y. Zhu, S.Q. Zhang, H.B. Tang, H.M. Wang, Grain morphology evolution behavior of titanium alloy components during laser melting deposition additive manufacturing, Journal of Alloys and Compounds, 632 (2015) 505-513.
[30] Q. Zhang, J. Chen, X. Lin, H. Tan, W.D. Huang, Grain morphology control and texture characterization of laser solid formed Ti6Al2Sn2Zr3Mo1.5Cr2Nb titanium alloy, Journal of Materials Processing Technology, 238 (2016) 202-211.

Highlights

- Silicon addition decreases prior-β grain size in wire arc Additive Layer Manufactured (ALM) titanium.
- Cast alloys have smaller grains compared to the same alloys produced by ALM.
- Cyclical remelting during ALM destroys some equiaxed grains and favours epitaxial columnar growth.